Supporting Information:

Thermoelectric properties of n-type ZrNiSn prepared by rapid non-equilibrium laser processing

Yonggao Yan*[a]，Wuqian Geng[a]，Junhao Qiu[a]，Hongquan Ke[a]，Chuang Luo[a]，Jihui Yang[b]，Ctirad Uher[c]，Xinfeng Tang*[a]

[a]State Key Laboratory of Advanced Technology for Materials Synthesis and Processing, Wuhan University of Technology, Wuhan, Hubei 430070, China. E-mail: yanyonggao@whut.edu.cn; tangxf@whut.edu.cn

[b]Department of Materials Science and Engineering, University of Washington, Seattle, Washington 98195, USA

[c]Department of Physics, University of Michigan, Ann Arbor, Michigan 48109, USA

From the volatilization rate of Sn shown in figure 3a, Sn has the relatively higher volatilization rate than Zr and Ni. However, the value (the volatilization rate of Sn is only 0.014 g cm^{-2} s^{-1} at 2000 K) is still very low. Considering the speed of heating and cooling rate is more than 10^6 K/S during the SLM process, the melt lifetime is very short and the volatilization of Sn is greatly limited. The observation of Sn as a second phase could be correlated to the possible phase segregation from half-heusler ZrNiSn to full heusler $ZrNi_2Sn$, Sn and Zr. However, Zr exist in the form of ZrO_2, which could be seen from the SEM photo give below. The ZrO_2 particle tends to migrate to the surface of the ZrNiSn layer, and was removed by polishing during the SLM process.

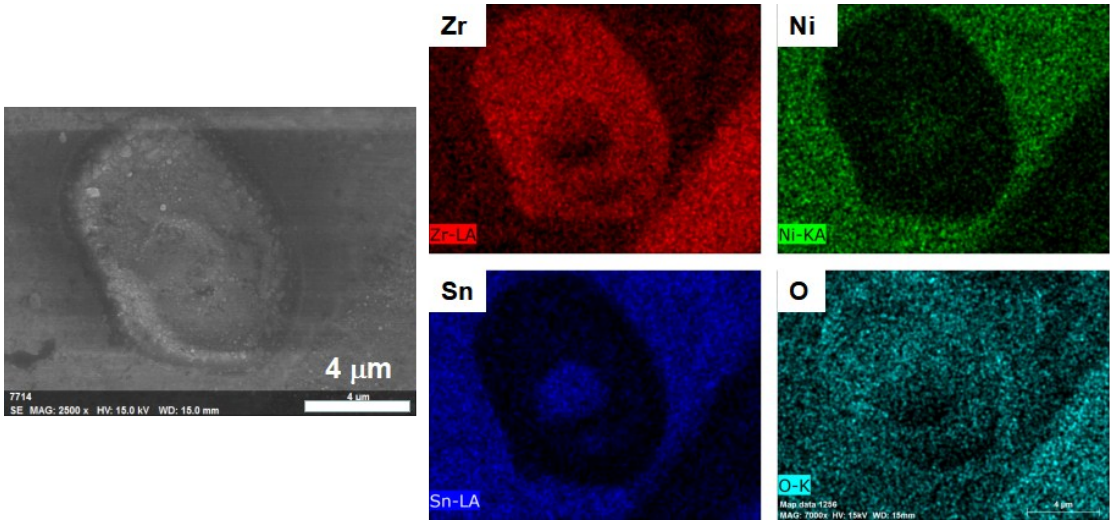

Figure S1. SEM photo shows ZrO2 particles on the SLM-prepared layer surface

Based on our room temperature Hall coefficient measurements, the carrier density of the SHS-SLM sample (7.54×10^{20} cm^{-3}) is an order of magnitude higher than the SHS- SPS sample (5.87×10^{19} cm^{-3}). The powder prepared by SHS shows single phase, and after the SPS process, the samples can remain phase purity. However, based on our XRD results, during the SLM process, Sn tends to migrate out from the ZrNiSn lattice to form a second phase in the SLM-prepared sample. The ZrNiSn matrix of

SLM-prepared sample must contains more Sn vacancy sites and Zr/Sn antisite defects than the SHS-SPS prepared sample, both leading to a much higher carrier density as observed. To further confirm the Sn content percentage in the sample prepared by SLM, DSC curve up to 673 K was collected and the Sn content was calculated using the intensity of peak due to Sn melting. The atomic percentage of Sn in the SLM-prepared samples is 5.87 %.

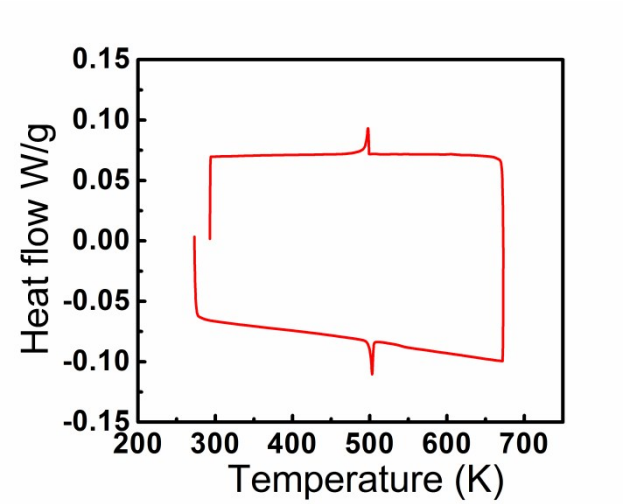

Figure S2. DSC of the SHS-SLM sample after annealing

The heat capacity C_p of the SLM-prepared sample was measured from 273 K to 450 K as shown in the following figure. The C_p value is calculated using sapphire as a standard reference. The C_p of the SLM-prepared ZrNiSn increased from 0.285 J/K at 273 K to 0.31 J/K at 450 K. When the temperature increase further, the C_p value is expected to be a constant according to Dulong-Petit law. The Dulong-Petit heat capacity is calculated to be 0.278 J/K, which is marginally lower than the measured C_p. The measured C_p and the figure will be included in the revised manuscript as the supplementary Information.

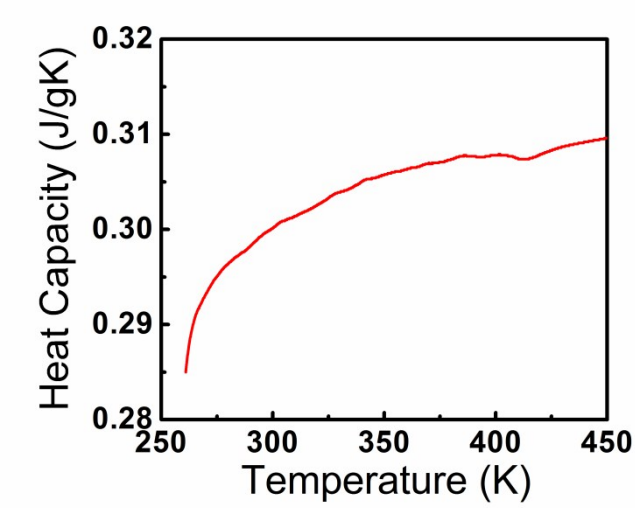

Figure S3. Measured C_p of the SHS-SLM prepared sample by DSC

The measured carrier concentration and Hall mobility of the SHS-SPS sample, and the SHS-SLM sample (before and after annealing) are listed in the table S1 below. As the reviewer mentioned, the mobility of the as-prepared SHS-SLM sample is very low compared with the SHS-SPS prepared

sample, due to the fact that the SHS-SLM sample contains a lot of Zr/Sn antisite defects, second phase Sn, smaller grain size (figure 6) and also micro-cracks (figure 4c and 4d). After annealing, the sample actually becomes more uniform according to the Seebeck coefficient mapping (figure S4), therefore the carrier concentration in the annealed sample decreases and the mobility increases, also possibly due to the eliminated micro-crack and enlarged grain size.

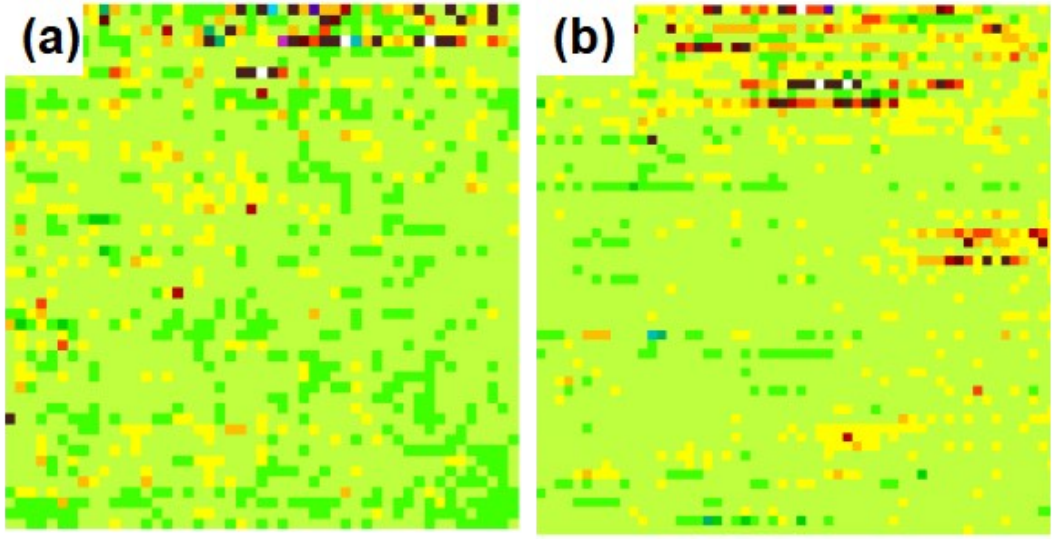

Figure S4. Seebeck coefficient mapping of the SLM-processed samples: (a) as-prepared; and (b) annealed.

Table S1. Some transport properties of the samples prepared by SPS and SLM process

Sample	n_H (10^{20} cm^{-3})	μ (cm^{2}V^{-1}K^{-1})	α(μVK^{-1})	κ (W m^{-1} K^{-1})
SHS-SPS	0.59	21.2	-248	6.01
SHS-SLM(as prepared)	7.54	1.02	-61	3.66
SHS-SLM(after annealing)	2.13	11.3	-63	3.74

The following figure S5 show the interface of ZrNiSn with Ti substrate prepared by SHS-SLM before & after annealing at 500℃ for 24 h, respectively. After annealing, the interphase layer thickness does not change and are around 5 μm. A slight diffusion of Ti into ZrNiSn can be observed, as highlighted by the blue rectangular.

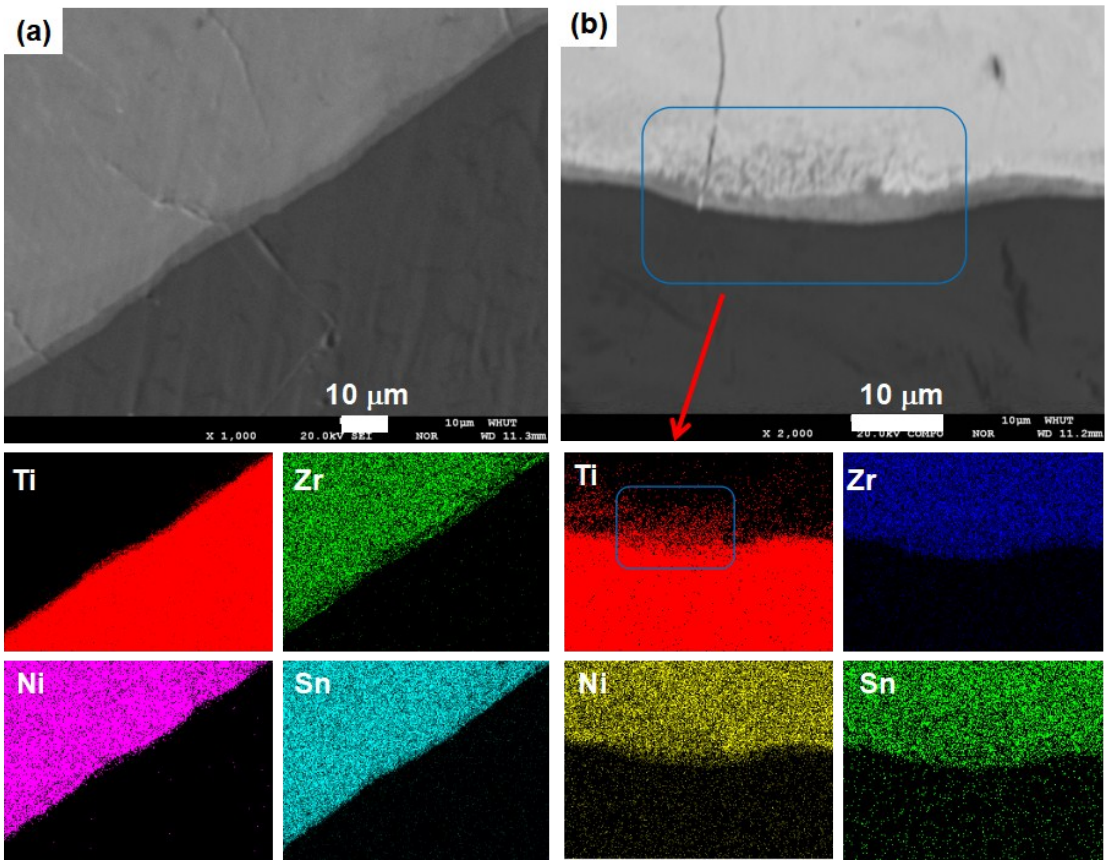

Figure S5. Backscattering electron images of the interface of SLM-prepared ZrNiSn on Ti substrate. (a) as-prepared; (b) annealed at 450 °C for 24 hours.

The interphase layer shows a Ti-rich composition close to $Zr_{5.86}Ni_{14.81}Sn_{12.80}Ti_{65.53}$, while after annealing, the interphase composition changes very slightly as shown in figure S6.

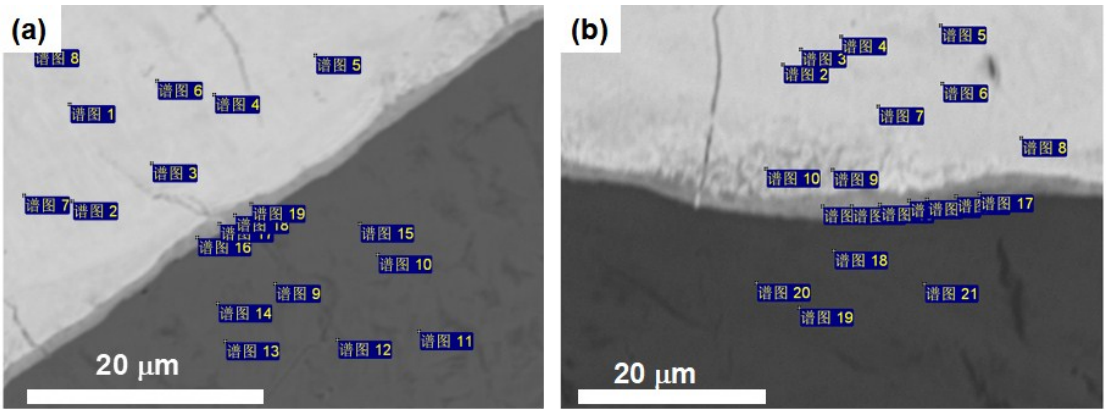

	Zr (%)	Ni (%)	Sn (%)	Ti (%)
16	5.8	16.68	10.67	66.85
17	5.3	13.28	13.51	67.91
18	5.75	15.16	12.89	66.21
19	6.06	14.10	14.12	65.72
Aver	5.86	14.81	12.80	65.53

	Zr (%)	Ni (%)	Sn (%)	Ti (%)
11	5.63	14.28	11.67	64.87
12	6.08	17.49	13.24	63.19
13	8.84	17.73	13.05	59.38
14	7.18	14.54	13.75	64.53
Aver	6.88	15.99	13.18	63.95

Figure S6. The EPMA results for the SLM-prepared ZrNiSn: (a) as-prepared; (b) annealed at 450 °C for 24 hours.

As we mentioned above, the interphase layer shows a Ti-rich composition close to $Zr_{5.86}Ni_{14.81}Sn_{12.80}Ti_{65.53}$, while after annealing, the interphase composition changes very slightly. The thickness of interface layer is around 5 μm as observed from the EDS line scan result shown in the figure S7 below.

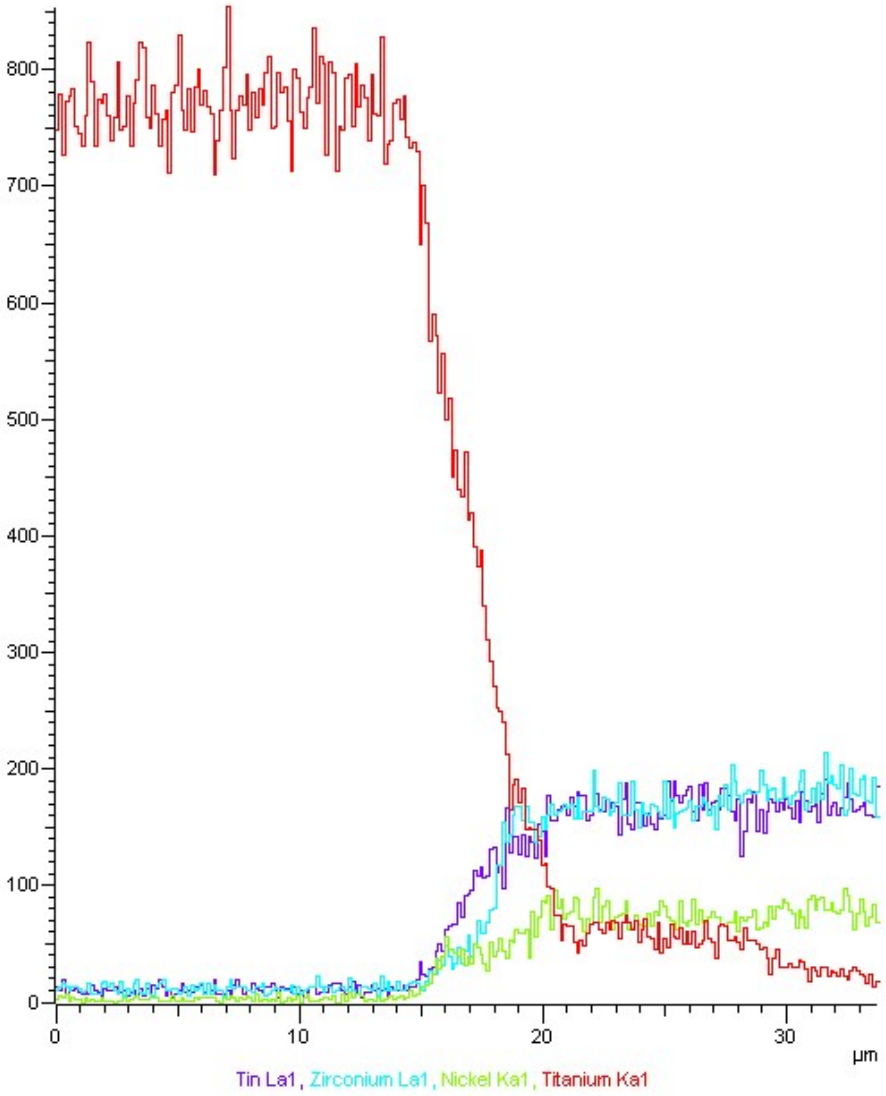

Figure S7. EDS line scanning map of the cross-section of SHS-SLM ZrNiSn with Ti substrate after annealing

The joining of ZrNiSn and metal substrate can be considered as laser welding. Only when the two materials have similar melting points and coefficients of thermal expansion, can they form a suitable bonding. By a survey on common metals as shown in Table S2, Ti shows a close melting point and a similar coefficient of thermal expansion to ZrNiSn. Therefore, we select Ti as the proper electrode for ZrNiSn to ensure good bonding.

Table S2. Basic parameters of different metal electrodes

	Melting point（℃）	thermal expansion coefficient（10^{-6}/℃）
Sn	232	19.5
Ni	1453	12
Cu	1083	17.1
Ti	1675	9
Al	660	23.6
ZrNiSn	1435	9.8